

Single-Pion Production in Neutrino-Nucleus Interactions in the Few-GeV Region

Makoto Sakuda ^{a*} and Emmanuel A. Paschos ^{b†}

^aKEK, Institute of Particles and Nuclear Studies,
Oho 1-1, Tsukuba,305-0801, Japan

^bUniversitat Dortmund, Institut fur Physik,
D-44221 Dortmund, Germany

We review the existing experimental data and models of single-pion production in neutrino-nucleus interactions in the few-GeV region. We mainly discuss the effect of Pauli exclusion effect and the $N\Delta$ vector form factors, which were not properly considered before. We propose the new direction for modelling single-pion production.

1. Introduction

Many neutrino oscillation experiments have been proposed in the few-GeV region after atmospheric neutrino oscillations and solar neutrino oscillations become established[1]. Precise knowledge of neutrino-nucleus interactions in this energy region is becoming more important in neutrino experiments. In the few-GeV region, the cross section of single-pion production is as large as the quasi-elastic cross section. Various resonances seen in the $\gamma - N$ and $\pi - N$ system should be present in the invariant-mass (W) spectra of single-pion production in neutrino interactions. $\Delta(1232)$ is the dominant resonance in single-pion production and there are other prominent resonances, like $P_{11}(1440)$, $D_{13}(1520)$, $S_{11}(1535)$, $F_{11}(1680)$ and $P_{13}(1740)$ below $W < 2$ GeV. Furthermore, a non-resonant process, like deep-inelastic scattering, begins to contribute to single-pion production as the energy increases. We review the models of single-pion production in neutrino-nucleus interactions based on the most updated knowledge of electron- and neutrino-nucleus scattering, and propose some features to improve the models.

2. Experimental data of single-pion production

Previous measurements of single-pion production were performed by the Bubble Chamber experiments for the charged-current (CC) processes, and are plotted in Figs.1-3: $\nu_\mu + p \rightarrow \mu^- + p + \pi^+$ [2-5,7,6], $\nu_\mu + n \rightarrow \mu^- + p + \pi^0$ [3,4,7], $\nu_\mu + n \rightarrow \mu^- + n + \pi^+$ [3,4], $\bar{\nu}_\mu + n \rightarrow \mu^+ + n + \pi^-$ [7,8], and $\bar{\nu}_\mu + p \rightarrow \mu^+ + p + \pi^-$ [7,4]. The cross section increases with the incident neutrino energy above 0.5 GeV and saturates as the energy increases above 5 GeV. As can be seen in the plots, the cross sections vary at the level of 20-30%, mainly due to the flux uncertainty of the wide-band neutrino beams. BNL and ANL Bubble Chamber groups [3,4] showed that the $I=1/2$ amplitude is comparable in size to the $I=3/2$ amplitude in the reactions of $\mu^- + p + \pi^0$ and $\mu^- + n + \pi^+$ and that the $I=1/2$ amplitude becomes even comparable at the high-mass region. Furuno of the BNL Bubble Chamber group [9] at this workshop showed the ratio of the cross section of single pion production to the quasi-elastic scattering in order to reduce the systematic error due to the uncertainty of the flux (Fig.4).

The $d\sigma/dQ^2$ distribution is very fundamental in the cross-section measurement and calculation, where $Q^2 = -(q_1 - q_2)^2$ is the four-momentum transfer squared. The Q^2 distribution of the

*makoto.sakuda@kek.jp

†paschos@physik.uni-dortmund.de

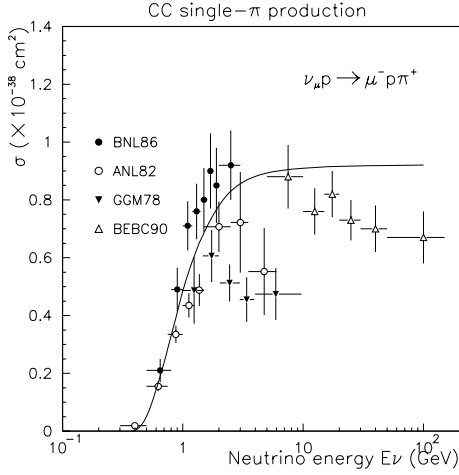


Figure 1. Cross sections for single-pion production $\nu_\mu + p \rightarrow \mu^- + p + \pi^+$ [2-5,7,6]. Gargamelle data[2] are given for $W < 1.4 \text{ GeV}/c^2$. Other data do not use W cut. The solid curve represents a calculation of the Rein-Sehgal model [12] with $M_A = 1.2 \text{ GeV}/c^2$.

$\mu^- p \pi^+$ channel was also presented by Furuno [9] at this workshop (Fig.5). Figs.6(a-b) show the Q^2 distribution in (a) a charged-current quasi-elastic enhanced sample and (b) a charged-current inelastic enhanced sample in K2K [11]. Monte Carlo prediction is shown in boxes. In the few-GeV region inelastic events are dominated by the single-pion production, as seen in Fig.6(c). The shadowed area is due to single-pion production and the black area is due to quasi-elastic events.

A K2K experiment showed the preliminary result on NC single π^0 production at the previous NuInt01 workshop [10], which is dominated by NC resonance production. Their inclusive π^0 momentum distribution is shown in Fig.7.

3. Models of single-pion production

The model of Rein-Sehgal [12] is commonly used to calculate single-pion production by many neutrino experiments. This model is based on the relativistic harmonic oscillator quark model of

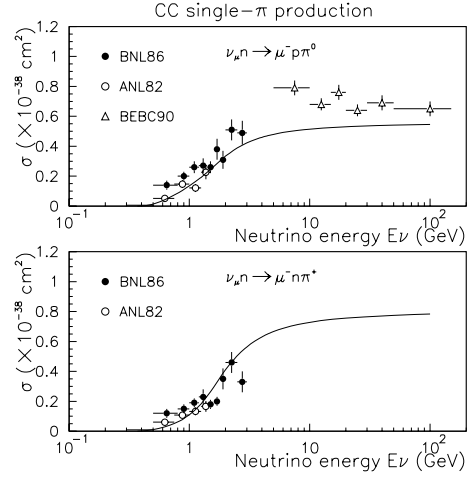


Figure 2. Cross sections for single-pion production $\nu_\mu + n \rightarrow \mu^- + p + \pi^0$ [3,4,7]. and $\nu_\mu + n \rightarrow \mu^- + n + \pi^+$ [3,4].

Feynman-Kislinger-Ravndal [13]. It naturally incorporates the contribution of baryon resonances (and their interferences) up to the invariant mass (W) of 2 GeV, which are described in SU(6) representations. It considers both the $I=3/2$ and $1/2$ charged current and neutral current. In this model, a nucleon is a ground state of a three-quark system tied together by harmonic forces, and any resonance N^* corresponds to the excited state. The vector and axial form factors for a resonance in the charged current are assumed to take the form

$$G^{V,A}(Q^2) = \left(1 + \frac{Q^2}{M_{V,A}^2}\right)^{-2} \cdot \left(1 + \frac{Q^2}{4M^2}\right)^{1/2(1-N)}, \quad (1)$$

where $M_{V,A}$ is the vector and axial vector mass and M is the nucleon mass. The first factor is a conventional dipole form and the second factor was introduced in a harmonic oscillator model [13]. N is the number of excitations of the resonances. For example, $N=0$ for $\Delta(1232)$, $N=1$ for $D_{13}(1520)$ and $S_{11}(1535)$, and $N=2$ for $P_{11}(1440)$. It is noted that the second factor makes the $\Delta(1232)$ vector form factor fall less rapidly than the dipole form factor. This dis-

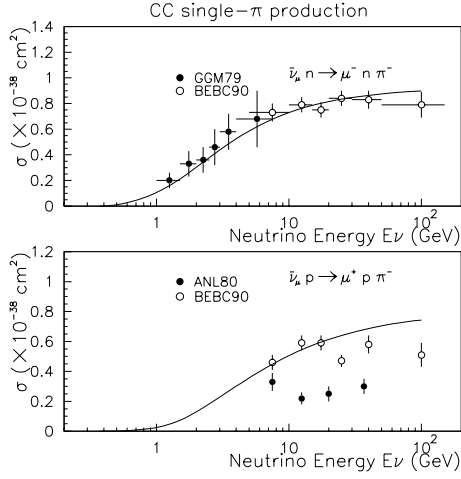


Figure 3. Cross sections for single-pion production $\bar{\nu}_\mu + n \rightarrow \mu^- + n + \pi^-$ [8,7] and $\bar{\nu}_\mu + p \rightarrow \mu^- + p + \pi^-$ [?, 7]. The Gargamelle data were corrected following the prescription of Ref.[7], $\sigma_{nucleon} = \sigma_{propane}/0.45$.

garees with the experimental data. The model also adds a non-resonant background contribution. We show the prediction of Rein-Sehgal model in Figs.1-5 in comparison with the experimental data. While we used $M_A = 1.2 \text{ GeV}/c^2$ in Figs.1-3, BNL data fit slightly better with $M_A = 1.1 \text{ GeV}/c^2$ [9]. Another popular model is one by Schreiner-von Hippel (SvH) [14]. The model starts with a general matrix element of $\nu_\mu + p \rightarrow \mu^- + \Delta^{++}$ in terms of spin-3/2 Rarita-Schwinger form factors as [15]

$$\begin{aligned} \frac{M}{\sqrt{3}} = & \frac{G}{\sqrt{2}} \bar{\psi}^\alpha \left[\left(\frac{C_3^V}{m_p} \gamma_\lambda + \frac{C_4^V}{m_p^2} (P_\Delta)_\lambda + \frac{C_5^V}{m_p^2} (P_p)_\lambda \right) \gamma_5 F^{\lambda\alpha} \right. \\ & + C_6^V j^\alpha \gamma_5 + \left(\frac{C_3^A}{m_p} \gamma_\lambda + \frac{C_4^A}{m_p^2} (P_\Delta)_\lambda \right) F^{\lambda\alpha} \\ & \left. + C_5^A j^\alpha + \frac{C_6^A}{m_p^2} (P_p)^\alpha q \cdot j \right] u f(W), \quad (2) \end{aligned}$$

where $q = q_1 - q_2$, j^α is the lepton-current matrix element, $F^{\lambda\alpha} = q^\lambda j^\alpha - q^\alpha j^\lambda$, ψ^α is the Rarita-Schwinger spinor describing the $\Delta(1232)$ spin state, u is the Dirac spinor describing the initial proton state and $f(W)$ is an s-wave Breit-Wigner term in the $\pi - N$ invariant mass (W) with $\Gamma=120 \text{ MeV}$. The SvH model uses the fol-

lowing form for the vector part:

$$\begin{aligned} C_3^V(Q^2) &= 2.05 \{ (1 + 9Q) \exp(-6.3Q) \}^{1/2}, \\ C_4^V &= -\frac{M}{W} C_3^V, \text{ and } C_5^V = C_6^V = 0. \quad (3) \end{aligned}$$

The form factor $C_3^V(Q^2)$ was determined by Dufner-Tsai [16] from an analysis of the Δ production in electron scattering. It considers the experimental observation that the Δ vector form factor falls more rapidly than the nucleon vector form factor, $(1 + Q^2/M_V^2)^{-2}$. See Fig.8 [17]. The axial form factors are assumed to take the following form:

$$C_5^A(Q^2) = 1.2 \left(1 + \frac{Q^2}{M_A^2} \right)^{-2} \left(1 - \frac{1.2Q^2}{2+Q^2} \right),$$

$$C_4^A = -C_5^A/4 \text{ and } C_3^A = 0. \quad (4)$$

Only $C_3^V(Q^2)$ and $C_5^A(Q^2)$ make a significant contribution to the cross section. Other form factors are negligible. The first term for $C_5^A(Q^2)$ is the dipole form factor, and the second factor was introduced to explain the Q^2 distribution of $\nu_\mu + p \rightarrow \mu^- + \Delta^{++}$ measured by ANL Bubble Chamber experiment [18], whose statistics was then about 150 events. Since the form factors are different in the above two models, it is natural that the M_V and M_A values determined by the models are different and cannot be compared.

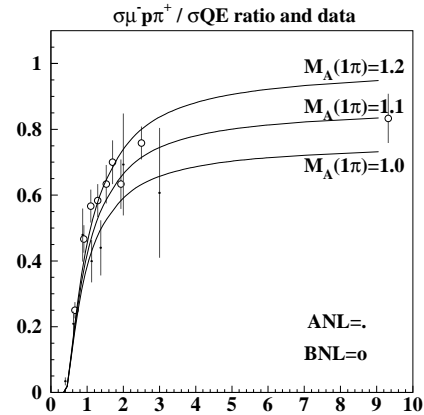


Figure 4. Cross-section ratio.

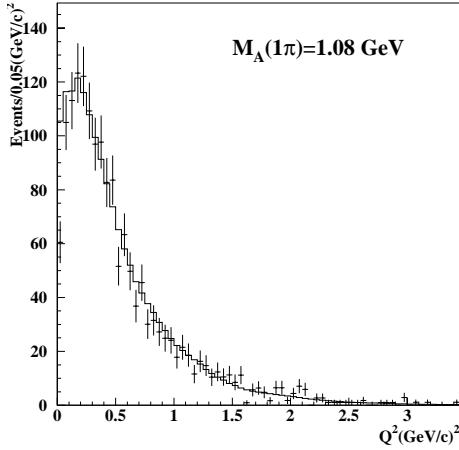


Figure 5. Q^2 distribution of $\nu_\mu + p \rightarrow \mu^- + p + \pi^+$ measured by the BNL experiment [3,9].

We now comment on the above two models. First, neither model considers the nuclear effect. Adler et al. [19] pointed out the effect of Pauli suppression in resonance production. For example, when the Δ^{++} resonance is produced in the nucleus through the reaction $\nu_\mu + p \rightarrow \mu^- + \Delta^{++}$, Δ decays hadronically into $p\pi^+$. The momentum value at the Δ rest frame is about 220 MeV/c. It is almost equal to the Fermi momentum (k_F) of the nucleons in carbon or oxygen. Depending on the decay angle of the proton with respect to the Δ production direction, the proton momentum in the laboratory frame can be less than k_F or greater than k_F . In the former case, the reaction is suppressed, since there are other protons in the nucleus with the momentum value less than k_F . In the latter case, the proton can emerge from the nucleus and the reaction is allowed. We show in Fig.9 the differential cross section $d\sigma/dQ^2$ for $\nu_\mu + p \rightarrow \mu^- + \Delta^{++}(\rightarrow p + \pi^+)$ at $E_\nu = 1.0$ GeV with (solid line) and without (dashed line) the Pauli suppression effect for the case of $k_F=225$ MeV/c. It shows that the suppression factor is about 10 – 20% in the low Q^2 region ($< 0.2(\text{GeV}/c)^2$). Fig.10 shows the the suppression factor, $G(W, Q^2, k_F)$, at different

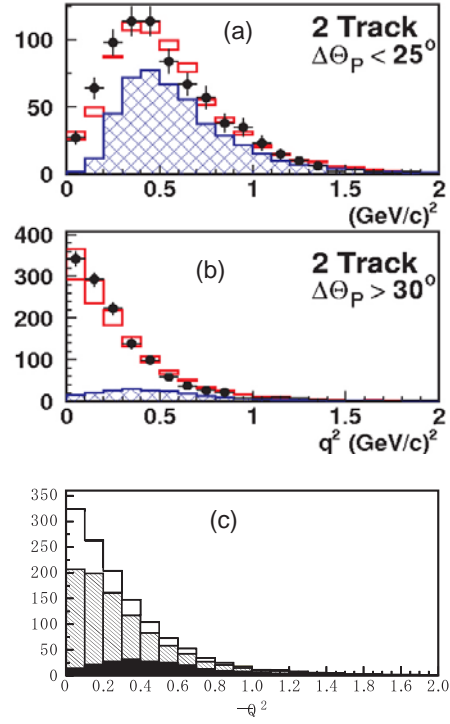


Figure 6. Q^2 distribution in (a) a charged-current quasi-elastic enhanced sample and (b) a charged-current inelastic enhanced sample in K2K [11]. Monte Carlo prediction is shown in boxes. The size of a box shows the uncertainty in the prediction. Figure (c) shows the content of the prediction. The shadowed area is due to the single pion production and the black area is due to quasi-elastic events.

invariant-mass W values. If the W value is lower (larger), the momentum value in the W rest frame is smaller (larger) and the suppression is larger (smaller), accordingly.

Secondly, we discuss the vector form factor for the Δ resonance. It is known experimentally that the $\Delta(1232)$ vector form factor falls more rapidly than the elastic form factors [16,17,21]. New measurement confirmed this point with better accuracy [22]. However, this feature was not considered seriously in calculating the resonance production in the neutrino-nucleus interaction.

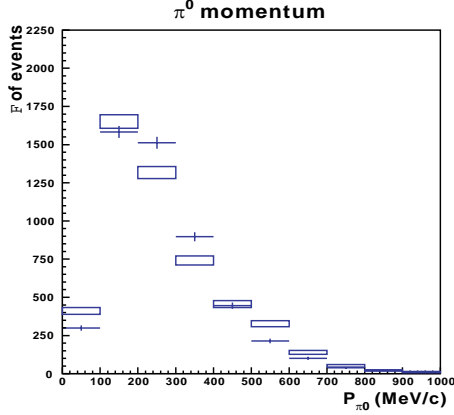


Figure 7. Momentum distribution of π^0 in $\nu_\mu + \text{water} \rightarrow \pi^0 + \text{Nothing}$ observed in the K2K 1kton detector.

Fig. 8 shows $[G_\Delta/G_D]^2$, where G_D is the dipole form factor, $(1 + Q^2/M_V^2)^{-2}$ ($M_V^2 = 0.71$). The data show that the correction for the vector form factor from a dipole form factor is about 0.95 at $Q^2 = 0.2$ (GeV/c^2), 0.84 at $Q^2 = 1.0$ (GeV/c^2) and 0.63 at $Q^2 = 2.0$ (GeV/c^2). The correction factor in Eq.(1) of Rein-Sehgal model is 1.03 at $Q^2 = 0.2$ (GeV/c^2) and 1.25 at $Q^2 = 2.0$ (GeV/c^2). This disagrees with the data. The corresponding factor in Eq.(3) of the SvH model is 0.9 at $Q^2 = 0.2$ (GeV/c^2) and 0.63 at $Q^2 = 2.0$ (GeV/c^2). We take this factor to be $(1 + \frac{Q^2}{3M_N^2})^{-1}$ for both vector and axial form factors [23], and it is 0.95 at $Q^2 = 0.2$ (GeV/c^2) and 0.64 at $Q^2 = 2.0$ (GeV/c^2). Our factor agrees with data. It is important that the vector form factor should be consistent with the recent data.

Considering the Pauli suppression factor, $G(W, Q^2, k_F)$, and the modified dipole form factors, we propose to use the following model. For $W < 1.6\text{GeV}/c^2$, a resonance model similar to the SvH model can be used:

$$C_i^{A,V}(Q^2) = C_i^{A,V}(0)G(W, Q^2, k_F)^{1/2} \cdot (1 + Q^2/M_{V,A}^2)^{-2} \cdot (1 + Q^2/(3M_N^2))^{-1}. \quad (i = 3, 4, 5) \quad (5)$$

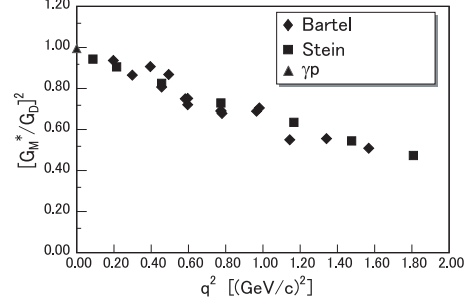


Figure 8. Scaled Δ form factor squared, $[G_\Delta/G_D]^2$, is plotted [17], where G_D is the dipole form factor, $(1 + Q^2/M_V^2)^{-2}$ ($M_V^2 = 0.71$).

We consider $\Delta(1232)$, $P_{11}(1440)$, $D_{13}(1520)$, and $S_{11}(1535)$ below $W < 1.6\text{GeV}/c^2$. Paschos et al.[20] already showed that this scheme may work. Above $W > 1.6\text{GeV}/c^2$, the contribution of deep inelastic scattering will be added [24]. A preliminary study with this form can be found elsewhere [23].

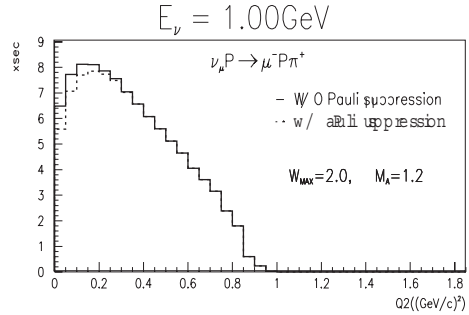


Figure 9. Cross section for $\nu_\mu + p \rightarrow \mu^- \Delta^{++} (\rightarrow P\pi^+)$ at $E_\nu = 1.0$ GeV with (dashed line) and without (solid line) Pauli suppression effect. $k_F = 220$ MeV/c is used.

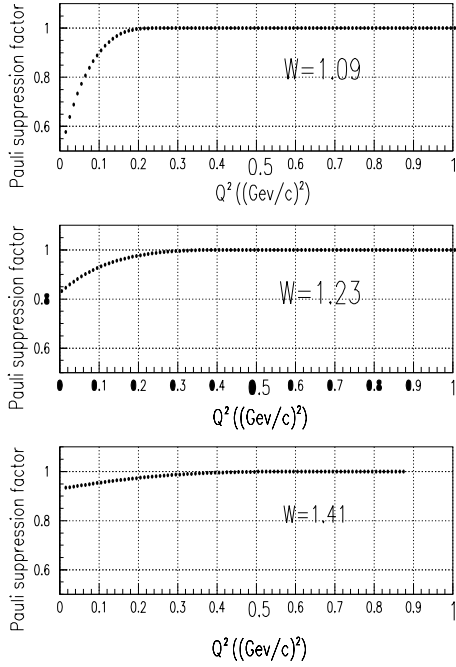


Figure 10. Pauli suppression factor $G(W, Q^2, k_F)$ with $W=1.04$, $W=1.23$ and $W=1.4$ GeV. $k_F=220$ MeV/c is used.

3.1. Summary

We have reviewed the existing experimental data and models of single-pion production in neutrino-nucleus interactions in the few GeV region. The accuracy of the cross section measurements are at the level of 20-30%. Single-pion production is dominated by the Δ resonance production in the few GeV region. We pointed out the effect of Pauli exclusion and the effect of the vector form factor in the calculation of Δ production cross section.

Recently, the nucleon electromagnetic form factors have been measured with good accuracy [25] and a clear deviation from a simple dipole parametrization, $(1 + Q^2/M_V^2)^{-2}$ with $M_V = 0.84$ (GeV/c)², has been observed. The better parametrizations for vector form factors were proposed [26,27]. The effect of those new form factors

on the neutrino quasi-elastic cross sections was shown to be a few % [28,29]. The $N\Delta$ vector form factor must be considered in calculation of the Δ resonance production to match the progress in the calculation of quasi-elastic cross section.

REFERENCES

1. D.L.Wark, Nucl.Phys.B(Proc.Suppl.)**117** (2003)164.
2. W. Lerche et al., Phys. Lett. **78B** (1978) 510.
3. T. Kitagaki et al., Phys. Rev. **D34** (1986) 2554.
4. G.M. Radecky et al., Phys. Rev. **D25** (1982) 1161.
5. P. Allen et al., Nucl. Phys. **B264** (1986) 221.
6. H.J. Grabosch et al., Z. Phys. **C41** (1989) 527; V.V. Ammosov et al., Sov. J. Nucl. Phys. **50(1)** (1989) 67. [Yad. Fiz. 50(1989)106.]
7. D.Allasia et al., Nucl.Phys.**B343**(1990)285.
8. T. Bolognese et al., Phys. Lett. **81B** (1979) 393.
9. K.Furuno, this Proceedings.
10. C.Mauger, Nucl. Phys. B(Proc.Suppl.)**112**(2002)146.
11. Y.Itow, this Proceedings; T.Ishida, this Proceedings.
12. D. Rein and L.M. Sehgal, Ann. Phys.(N.Y.) **133** (1981) 79; D.Rein, Z.Phys. **C35** (1987) 43.
13. R.P.Feynman, M.Kislinger and F.Ravndal, Phys.Rev.**D3**(1971)2706; F.Ravndal, Phys.Rev.D4(1971)1466.
14. P.A.Schreiner and F.von Hippel, Nucl. Phys. **B58**(1973)333.
15. C.H. Llewellyn Smith, Phys. Rep. **C3** (1972) 264.
16. A.J.Dufner and Y.S.Tsai, Phys. Rev. **168**(1968)1801.
17. W.Bartel et al., Phys.Lett.**B28**(1968)148; S.Stein et al., Phys.Rev.**D12**(1975)1884.
18. J.Campbell et al., Phys.Rev.Lett.**30**(1973)335.
19. S.L.Adler, S.Nussinov and E.A.Paschos, Phys.Rev. **D9** (1974) 2125.
20. E.Paschos, L.Pasquali and J-Y.Yu, Nucl.Phys. **B588**(2000)263.
21. G.Olsson et al., Phys.Rev.**D17**(1978)2938.

22. L.M.Stuart et al.,
Phys.Rev.**D58**(1998)032003.
23. E.Paschos, J-Y.Yu and M.Sakuda, hep-
ph/0308130, DOTH03001, August 2003.
24. A.Bodek and U-K.Yang, Nucl. Phys.
B(Proc.Suppl.)**112**(2002)70.
25. H.Gao, Int.J.Mod.Phys.**E12**(2003)1.
26. P.Bosted, Phys.Rev.**C51**(1995)409.
27. E.J.Brash et al.,
Phys.Rev.**C65**(2002)051001.
28. H.Budd, this Proceedings.
29. C.Walter, in Proceedings of NuFact03 Work-
shop, New York, May 2003.